International Journal of Nanomedicine

Dovepress
open access to scientific and medical research

Open Access Full Text Article

ORIGINAL RESEARCH

Enhanced osteogenic activity and anti-inflammatory properties of Lenti-BMP-2-loaded TiO_2 nanotube layers fabricated by lyophilization following trehalose addition

This article was published in the following Dove Press journal:
International Journal of Nanomedicine
25 January 2016
Number of times this article has been viewed

Xiaochen Zhang[1]
Zhiyuan Zhang[1]
Gang Shen[2]
Jun Zhao[2]

[1]Department of Oral and Maxillofacial Surgery, [2]Department of Orthodontics, College of Stomatology, Ninth People's Hospital, School of Medicine, Shanghai Jiao Tong University, Shanghai, People's Republic of China

Abstract: To enhance biocompatibility and osseointegration between titanium implants and surrounding bone tissue, numerous efforts have been made to modify the surface topography and composition of Ti implants. In this paper, Lenti-BMP-2-loaded TiO_2 nanotube coatings were fabricated by lyophilization in the presence of trehalose to functionalize the surface. We characterized TiO_2 nanotube layers in terms of the following: surface morphology; Lenti-BMP-2 and trehalose release; their ability to induce osteogenesis, proliferation, and anti-inflammation in vitro; and osseointegration in vivo. The anodized TiO_2 nanotube surfaces exhibited an amorphous glassy matrix perpendicular to the Ti surface. Both Lenti-BMP-2 and trehalose showed sustained release over the course of 8 days. Results from real-time quantitative polymerase chain reaction studies demonstrated that lyophilized Lenti-BMP-2/TiO_2 nanotubes constructed with trehalose (Lyo-Tre-Lenti-BMP-2) significantly promoted osteogenic differentiation of bone marrow stromal cells but not their proliferation. In addition, Lyo-Tre-Lenti-BMP-2 nanotubes effectively inhibited lipopolysaccharide-induced interleukin-1β and tumor necrosis factor-α production. In vivo, the formulation also promoted osseointegration. This study presents a promising new method for surface-modifying biomedical Ti-based implants to simultaneously enhance their osteogenic potential and anti-inflammatory properties, which can better satisfy clinical needs.

Keywords: osteogenesis, anti-inflammation, TiO_2 nanotube layers, Lenti-BMP-2, lyophilization, trehalose

Introduction

Titanium and its alloys are used extensively in developing dental and orthopedic implants due to their good biocompatibility, excellent corrosion resistance, and adequate mechanical properties.[1] However, Ti-based materials cannot facilitate sufficient osseointegration because of their suboptimal surface osteoconductivities.[2] Furthermore, the surfaces of Ti-based implants are prone to colonization by bacteria, and thus, lead to infections at implant sites. These are currently the two main reasons for implant surgery failure. Various surface modifications have been evaluated to overcome these problems and increase the success rates of Ti-based implants.

To enhance the biological performances of Ti-based implants, many studies have focused on surface modification methods such as plasma-spraying, sandblasting, acid-etching, anodization, or calcium phosphate coatings.[3,4] Among these methods, surface nanocrystallization is believed to be an effective approach.[5] Nano-implants can enhance osteoblast function in vitro and osseointegration in vivo more than

Correspondence: Jun Zhao; Gang Shen
Department of Orthodontics, College of Stomatology, Ninth People's Hospital, School of Medicine, Shanghai Jiao Tong University, 639 Zhizaoju Road, Shanghai 200011, People's Republic of China
Tel +86 21 6313 5412
Fax +86 21 6313 6856
Email yuzj_260@hotmail.com; gangshen@orthosh.com

conventional micro-implants.[6,7] TiO_2 nanotube layers formed by anodization have been widely studied and found to significantly promote bone formation.[8,9]

Coadministration of growth factors with TiO_2 nanotube implants may improve their osteoinductive capacity. Some scholars have demonstrated that the local delivery of appropriate bioactive molecules at favorable concentrations and rates can accelerate the process of osteogenesis.[10] Bone morphogenic proteins (BMPs) are a family of bone growth factors with a powerful ability to induce new orthotopic or ectopic bone formation.[11] Among them, BMP-2 is considered the most effective.[12,13] However, the local delivery of BMPs may have certain disadvantages, including short effective times, large dose requirements, the need for repeated administrations, high costs, and poor distribution profiles.[11] Fortunately, localized *BMP* gene therapy has emerged as a promising alternative approach for overcoming these shortcomings.[14] Because plasmid-based gene transfer is still inefficient, gene therapy based on viral vectors has been widely used to promote bone formation in a series of studies.[15,16] Among the various viral vectors available, lentiviral vectors can facilitate integration into the host genome in both dividing and nondividing cells, thus ensuring stable and long-term gene expression.[17] Moreover, lentiviral vectors have low immunogenicity,[18] and their safety has increased in recent years.[19] However, beyond the advantages, the use of lentiviral vectors also has several shortcomings. For example, lentiviral vectors may deliver inaccurate doses of growth factors, have uncontrolled flow, and be easily inactivated by heat, extreme pH, or proteases, which potentially destabilizes them during the therapeutic period.[20,21] Given these limitations, recent interest has emerged in coating biological molecules onto scaffolds via lyophilization.

Lyophilization, also known as freeze-drying, is an effective process that can overcome the instability of labile biopharmaceuticals.[22] Although this approach has been widely used to increase the physical and chemical stability of biopharmaceuticals, lyophilization generates a variety of stress during the freezing and desiccation processes, which can inactivate biomolecules to differing degrees.[23,24] Thus, protectants are often utilized to increase biomolecule stability during lyophilization.[25] Saccharides and disaccharides have been extensively and successfully used as nonspecific stabilizers to protect diverse biomolecules from inactivation during lyophilization. Trehalose, a nonreducing disaccharide consisting of two molecules of glucose, has been considered the most potent and widely studied protectant.[26] Compared with other stabilizers, trehalose exhibits some advantages such as a slower pH response, reducing the rates of acid fermentation and acid production.[27] In addition, trehalose inhibits inflammatory cytokine production induced by lipopolysaccharide (LPS).[28] Moreover, trehalose was found to significantly suppress excessive increases in the quantity of osteoclasts stimulated by LPS.[29] Collectively, these findings suggest the feasibility of functionalizing TiO_2 nanotube surfaces by combining trehalose and lyophilization treatment of lentiviral vectors encoding BMP-2, to produce nanotube layers with enhanced osteogenic and anti-inflammatory properties.

The objective of this study was to improve the osteoinductivity and anti-inflammatory properties of Ti-based implants by modifying their surfaces. To achieve this goal, TiO_2 nanotube layers formed by anodization were employed as substrates for growth factor delivery. A lentiviral vector encoding BMP-2 (Lenti-BMP-2) was loaded onto the nanotubes by lyophilization following trehalose addition. Different TiO_2 nanotube types were evaluated in terms of surface characteristics, release characteristics, inflammatory cytokine suppression, and their effects on osteogenic differentiation and proliferation of bone marrow stromal cells (BMSCs) in vitro and osseointegration in vivo.

Materials and methods

Preparation of TiO_2 nanotube layers

TiO_2 nanotube layers were prepared by anodizing thin Ti foils (0.25 mm thick, 99.5%) or Ti rods (2 mm in diameter and 8 mm in length), obtained from Alfa Aesar (Ward Hill, MA, USA). Briefly, the Ti foil or Ti rod was immersed for 5 minutes in a mixture containing 2 mL of 48% HF, 3 mL of 70% HNO_3 (both reagent-grade chemicals), and 100 mL of deionized water to remove the naturally occurring oxidation on the outer layer. The foil or rod was then rinsed in deionized water and dried in a nitrogen stream. TiO_2 nanotubes were fabricated with a potentiostat in an electrolyte solution containing 0.5% HF (w/v) and 1 M H_3PO_4, under a voltage of 20 V for 3 hours.[5] Anodic oxidation was performed at room temperature. After the nanotube layers had formed, the samples were rinsed and sonicated with deionized water and dried in a nitrogen stream. To crystallize the amorphous-structured TiO_2 nanotubes, the samples were then sintered at 500°C for 2 hours. All nanotubes used in this study were sterilized for 30 minutes in a steam autoclave at 120°C.

Preparation of coatings

Lenti-EGFP or Lenti-BMP-2 was produced by cotransfecting FUW (with *EGFP* or *BMP-2* gene), the HIV-1 packaging

vector Delta8.9, and VSVG envelope glycoprotein into 293T cell line, as described previously.[18] The human ubiquitin-C promoter in the FUW vector drives *EGFP* or *BMP-2* gene expression.[30] The woodchuck hepatitis virus posttranscriptional regulatory element (WPRE) is located downstream of inserted gene to increase its transcription. TOP10 bacteria were transformed with plasmids, and colonies were grown under ampicillin selection. For the lyophilization groups, solutions containing Lenti-BMP-2-EGFP or Lenti-EGFP particles (10^{11}/mL) mixed with an equal volume of 1 M trehalose (Lyo-Tre-Lenti-BMP-2-EGFP or Lyo-Tre-Lenti-EGFP) or 1 M trehalose alone (Lyo-Tre) were dropped onto the TiO_2 nanotube surfaces at a fixed volume of 30 µL/sample. The samples were then prefrozen at −80°C for 3 hours and lyophilized for 24 hours in a FreeZone freeze-drier (Labconco, Kansas City, MO, USA). TiO_2 nanotubes that did not undergo lyophilization were used as a control group (TiO_2).

Scanning electron microscopy

All scanning electron microscopy (SEM) images were taken with a Quanta 200 field-emission gun SEM (SEM XL-30; Philips, Amsterdam, the Netherlands). The Schottky field-emission gun enabled high spatial resolution. All samples were sputtered with platinum for 1 minute before imaging and mounted on sample holders with conductive carbon tape.

In vitro Lenti-BMP-2 and trehalose-release studies

To determine the release kinetics of Lenti-BMP-2 and trehalose from TiO_2 nanotube surfaces, samples were washed with phosphate-buffered saline and incubated at 37°C in six-well plates, containing 1 mL of Dulbecco's Modified Eagle's Medium (DMEM) with 10% fetal bovine serum (FBS) per well. DMEM and FBS were obtained from Gibco BRL (Grand Island, NY, USA) and Hyclone (Logan, UT, USA), respectively. The medium was sampled at 1, 6, 12, and 24 hours and 2, 4, 6, and 8 days. The release of Lenti-BMP-2 over time was determined by infecting 293T cells with 10 µL of supernatant taken from the six-well plate at each time point. EGFP-positive cells were counted at 3 days post-infection. To monitor the release of trehalose, separate medium samples (10 µL) were taken at each time point and analyzed on a high-performance liquid chromatography system (Waters, Milford, MA, USA), per the manufacturer's instructions. The high-performance liquid chromatography setup comprised a guard column attached to the analytical column (Sugar Pak: 6.5×300 mm), equipped with a reflective index detector (RID-2410). The oven was heated to 70°C, and Ca^{2+}/ethylenediaminetetraacetic acid was used as the mobile phase with a constant flow rate of 0.4 mL/min. Trehalose release into the DMEM samples was analyzed, and the amount of trehalose present in the nanotube layers was calculated.

Culture of rat BMSCs

Six-week-old male Fisher 344 rats were obtained from the Ninth People's Hospital Animal Center in Shanghai, People's Republic of China. All animal-handling procedures were carried out in accordance with, and the experimental protocol for this study was approved by, the Animal Care and Experiment Ethics Committee of the Ninth People's Hospital, which is affiliated with the Shanghai Jiao Tong University Medical School. Rat BMSCs were isolated and cultured at 37°C and 5% CO_2 in DMEM containing 10% FBS and 100 units/mL of penicillin and streptomycin, as described.[31] BMSCs were passaged two times before being used.

Effect on BMSCs osteogenic differentiation

The osteogenic differentiation of BMSCs cocultured with different treatment groups (TiO_2, Lyo-Tre, Lyo-Tre-Lenti-EGFP, and Lyo-Tre-Lenti-BMP-2-EGFP) in six-well transwell plates (0.4 µm; Corning Incorporated, Corning, NY, USA) was monitored on days 2, 4, and 8. Total RNA was extracted with the Trizol Plus RNA Purification Kit (Invitrogen, Carlsbad, CA, USA) according to the manufacturer's instructions. Highly purified gene-specific primers for Runx2, OPN, OCN, BSP, and the reference *GAPDH* gene were synthesized commercially (Shengong, Co., Ltd., Shanghai, People's Republic of China). Sequences of the primer sets used are outlined in Table 1. The expression levels of each bone marker gene and GAPDH were measured in three independent experiments by real-time quantitative polymerase chain reaction with a 7900HT sequence-detection system (Applied Biosystems, Foster City, CA, USA). Gene expression analysis was performed by calculating the relative expression levels of endogenous bone marker genes relative to those in BMSCs cocultured with TiO_2. Results are reported as the mean ± standard deviation.

Effect on BMSCs proliferation

The proliferation of BMSCs cocultured with different nanotube formulations was determined in six-well transwell plates (0.4 µm; Corning Incorporated). BMSCs were seeded at 10^5 cells/well in the lower wells, and the medium was changed every 2 days. On days 1, 2, 4, and 8, BMSCs were

Table 1 Nucleotide sequences of primers used for RT-qPCR

Genes	Primer sequence (5′–3′) (forward/reverse)	Product size (bp)	Annealing temperature (°C)	Accession number
Runx2	TCTTCCCAAAGCCAGAGCG/TGCCATTCGAGGTGGTCG	154	60	NM_053470.1
OPN	CCAAGCGTGGAAACACACAGCC/GGCTTTGGAACTCGCCTGACTG	165	60	NM_012881
OCN	CAGTAAGGTGGTGAATAGACTCCG/GGTGCCATAGATGCGCTTG	172	60	NM_013414.1
BSP	TGGATGAACCAAGCGTGGA/TCGCCTGACTGTCGATAGCA	162	60	NM_012881.2
GAPDH	GGCAAGTTCAACGGCACAGT/GCCAGTAGACTCCACGACAT	76	60	NM_017008.3

Abbreviations: RT-qPCR, real-time quantitative polymerase chain reaction; bp, base pair.

collected, and DNA contents were quantified to measure proliferation using the dye Hoechst 33258 (Sigma, St Louis, MO, USA), as previously described.[32]

Measurement of IL-1β and TNF-α

To analyze the potential anti-inflammatory properties of trehalose, mouse macrophage RAW 264.7 cells (Chinese Academy of Science Cell Bank, Shanghai, People's Republic of China) were seeded at 10^5 cells/well in the presence of LPS (5 μg/mL) in the lower wells of a six-well transwell culture system (0.4 μm; Corning Incorporated). Subsequently, different groups (TiO_2, Lyo-Tre, Lyo-Tre-Lenti-EGFP, and Lyo-Tre-Lenti-BMP-2-EGFP) were added to the upper wells. We used commercial enzyme-linked immunosorbent assay kits (BioSource International, Inc., Camarillo, CA, USA) to quantify interleukin-1β (IL-1β) and tumor necrosis factor-α (TNF-α) production in the cell-free culture supernatants after 12 hours, following the manufacturer's protocols. The absorbance at 450 nm was measured using a Multiskan JX microplate reader (Version 1.1; Thermo Labsystems Oy, Vantaa, Finland). The lower wells containing cells with added LPS or untreated cells were used as positive or negative controls, respectively.

In vivo osseointegration evaluation

Surgical procedure

Twenty-four male, Fisher 344 rats with bilateral femurs were used for the implantation of the following four groups of implants: (A) the TiO_2 group (n=12), (B) Lyo-Tre group (n=12), (C) Lyo-Tre-Lenti-EGFP group (n=12), and (D) Lyo-Tre-Lenti-BMP-2-EGFP group (n=12).

Sample preparation

At 8 weeks postsurgery, all Fisher 344 rats were sacrificed, and their bilateral femurs were harvested. Six specimens per group were randomly selected and fixed in 10% buffered formaldehyde for histomorphometric observations. The remaining six specimens were stored at −80°C for push-out tests.

Histomorphometric observations

Randomly selected specimens were dehydrated with a graded ethanol series, ranging from 50% to absolute ethanol, and then embedded in polymethylmethacrylate for undecalcified sectioning. The embedded specimens were sectioned into 150 μm thick sections in an orientation nearly parallel to the long axis of the implants, using a Leica SP1600 saw microtome (Leica, Wetzlar, Germany). Next, the sections were grounded and polished to final thickness of ~30 μm. Finally, the specimens were stained with Van Gieson's picro fuchsin for histological observations. The area of newly formed bone around the implants and the percentage of bone–implant contact (BIC) were evaluated with Image-Pro Plus 6.0 software (Media Cybernetics, Rockville, MD, USA).

Biomechanical testing

The push-out test was performed using a universal material testing system (Instron Ltd., High Wycombe, UK). All tests were performed using a loading rate of 5 mm/min. Load–displacement curves were recorded during the pushing period. The failure load was defined as the peak load value for each load–displacement curve.

Statistical analysis

All statistical analyses were performed using the SAS 8.2 statistical software package (SAS, Cary, NC, USA). *P*-values <0.05 were considered statistically significant.

Results

SEM studies

The surfaces of pure Ti exhibited shallow grooves and small grain sizes owing to machining and polishing in Figure 1A (Ti). The anodized TiO_2 nanotubes were nearly perpendicular to the substrate surface, and the layer was uniform in Figure 1B (TiO_2). The amorphous glassy matrix remaining on the surfaces of the anodized nanotube layers is shown in Figure 1C (Lyo-Tre) and Figure 1D (Lyo-Tre-Lenti-EGFP and Lyo-Tre-Lenti-BMP-2-EGFP). The cross-sections obtained from mechanically cracked samples of TiO_2 and

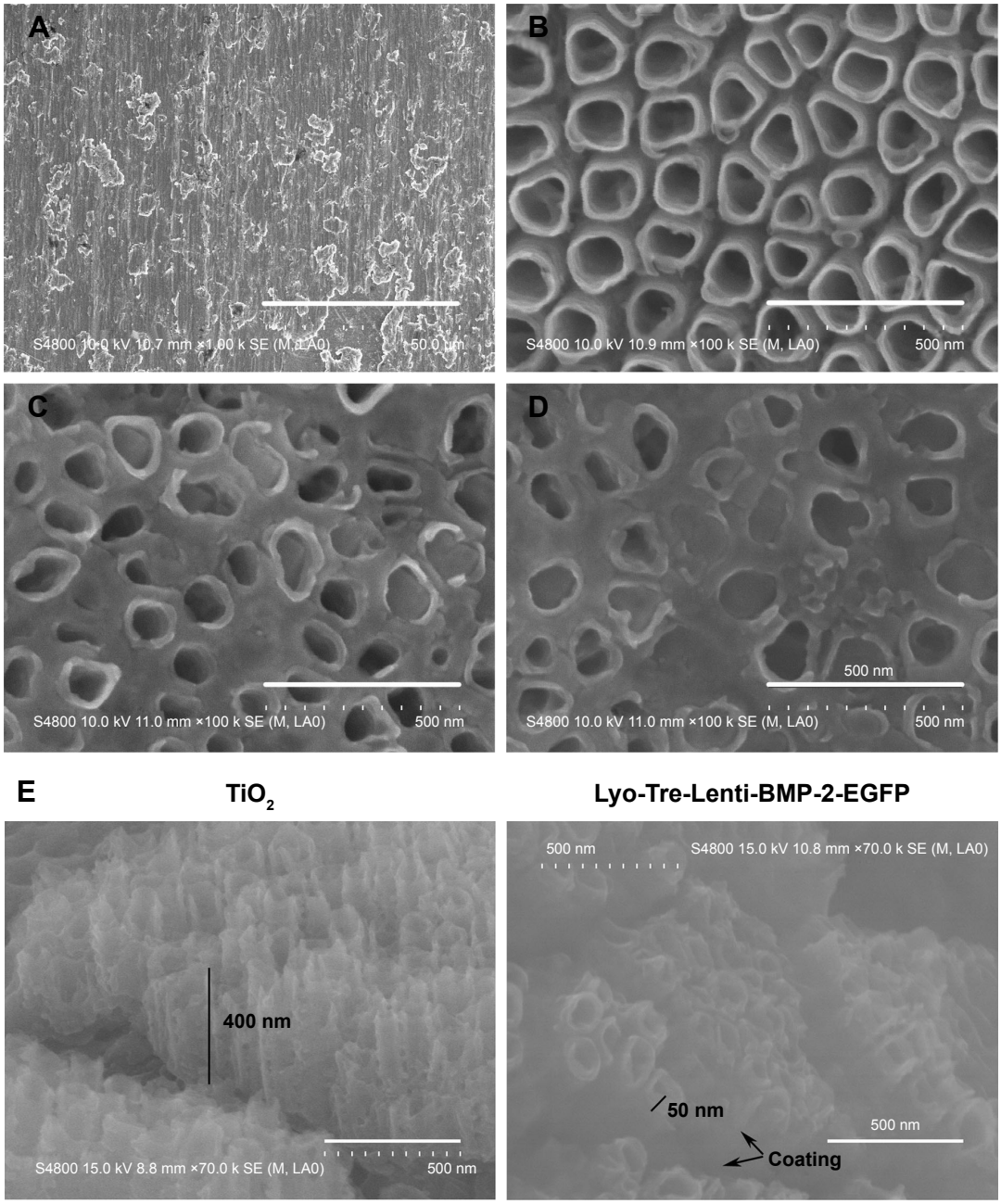

Figure 1 SEM micrographs of pure Ti and TiO_2 nanotube layers fabricated by anodization with different modifications.
Notes: (**A**) Smooth Ti. (**B**) TiO_2 nanotubes. (**C**) Lyo-Tre nanotubes. (**D**) Lyo-Tre-Lenti-BMP-2-EGFP or Lyo-Tre-Lenti-EGFP nanotubes. (**E**) Cross-sections of TiO_2 and Lyo-Tre-Lenti-BMP-2-EGFP nanotubes.
Abbreviations: SEM, scanning electron microscopy; BMP, bone morphogenic protein.

Lyo-Tre-Lenti-BMP-2-EGFP are shown in Figure 1E. Thickness of the nanotube layers was ~400 (TiO_2) and 50 nm (Lyo-Tre-Lenti-BMP-2-EGFP), indicating that the Tre-Lenti-BMP-2-EGFP coating was ~350 nm and uniform.

In vitro kinetics of Lenti-BMP-2 and trehalose release from TiO_2 nanotubes

The in vitro Lenti-BMP-2 release profile is shown in Figure 2A. Lyophilized Lenti-BMP-2 added to TiO_2 nanotubes showed a sustained release, exhibiting an initial burst of >50% on the first day, followed by a more gradual release from day 2 to 8. The cumulative release of trehalose over the 8-day period is shown in Figure 2B. When trehalose was added to the nanotube layers as a protectant against the lyophilization process, an initial burst release of >65% was observed during the first day, followed by a declining release rate until the end of the observation period.

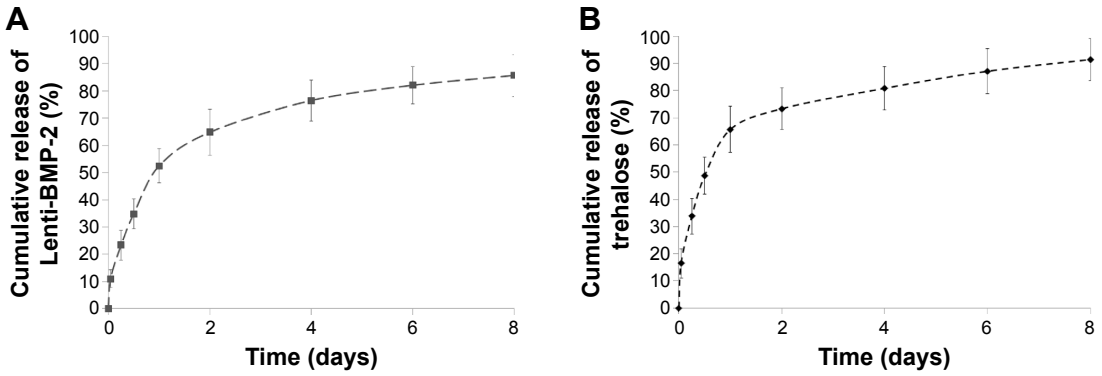

Figure 2 In vitro release profiles of Lenti-BMP-2 and trehalose.
Note: (**A**) In vitro Lenti-BMP-2- and (**B**) trehalose-release profiles.
Abbreviation: BMP, bone morphogenic protein.

Effect of different nanotube formulations on BMSCs osteogenic differentiation

The osteogenic differentiation of BMSCs cocultured with different nanotube formulations was determined by real-time quantitative polymerase chain reaction (Figure 3). For the Lyo-Tre-Lenti-BMP-2-EGFP group, the mRNA expression of Runx2 and OPN showed an initial upregulation at day 2, which increased continuously from day 4 to 8. BSP and OCN expression showed a slight rise between day 2 and 4 and was then dramatically enhanced from day 4 to 8. For the Lyo-Tre-Lenti-EGFP, Lyo-Tre, and TiO_2 groups, the mRNA expression levels of Runx2, OPN, BSP, and OCN were similar, with no significant difference in expression levels observed at any time point. However, osteogenic marker mRNA expression levels following incubation with Lyo-Tre-Lenti-EGFP, Lyo-Tre, and TiO_2 nanotubes were significantly lower ($P<0.05$) at days 2, 4, and 8, compared to that observed in cells treated with Lyo-Tre-Lenti-BMP-2-EGFP.

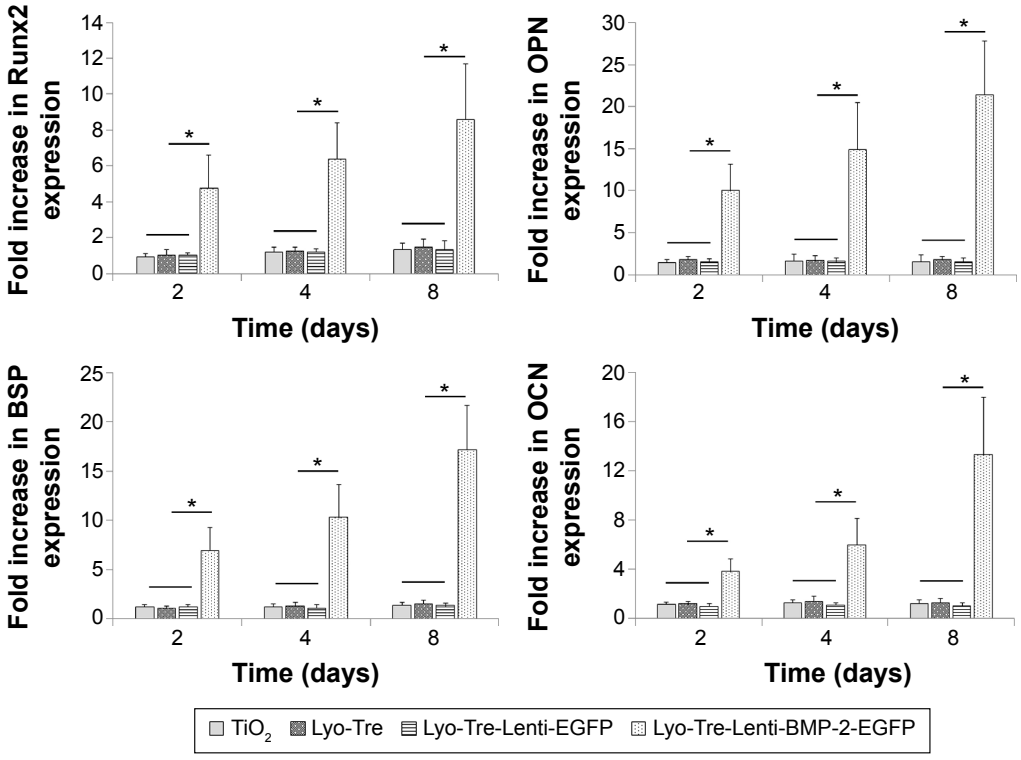

Figure 3 Effects of different nanotube formulations on the osteogenic differentiation of BMSCs.
Notes: RT-qPCR analysis of gene expression of osteogenic markers, including Runx2, OPN, BSP, and OCN in BMSCs cocultured with various nanotube types for 2, 4, and 8 days. All mRNA expression values were normalized to GAPDH mRNA expression. Stars and lines indicate significant differences between groups at each time point ($P<0.05$).
Abbreviations: BMP, bone morphogenic protein; BMSCs, bone marrow stromal cells; RT-qPCR, real-time quantitative polymerase chain reaction; GAPDH, glyceraldehyde-3-phosphate dehydrogenase.

Furthermore, from day 2 to 8, no obvious increase in the mRNA expression levels of Runx2, OPN, BSP, and OCN in BMSCs treated with these three groups was found.

Effect of different nanotube formulations on BMSCs proliferation

The proliferation of BMSCs cocultured with different groups was determined by performing a DNA-detection assay, as shown in Figure 4. Cellular proliferation following coculture with medium only, TiO_2, Lyo-Tre, Lyo-Tre-Lenti-EGFP, or Lyo-Tre-Lenti-BMP-2-EGFP was nearly identical at each time point. After coculture for 8 days, no significant differences in cell proliferation were observed with any of these four different TiO_2 nanotube types, relative to cellular proliferation observed with medium control cells.

Inhibitory effects of trehalose on LPS-induced IL-1β and TNF-α production

We found that production of both IL-1β and TNF-α in culture supernatants increased upon LPS stimulation (Figure 5). Although IL-1β production in LPS-stimulated cells was higher than observed with negative-control cells, IL-1β induction was inhibited by trehalose (Figure 5A). We also found that trehalose strongly inhibited LPS-induced TNF-α production (Figure 5B).

Histological analysis

As shown in Figure 6A, a rectangular region (1.5×0.5 mm) adjacent to the epiphyseal plate and around the implant surface was chosen to evaluate new bone formation. The detail of the bone–implant interface is shown with the Van Gieson's picro fuchsin staining sections (Figure 6B). In the TiO_2 group, an obvious interspace between the newly formed bone and the implant surface was filled with fibrous tissue. Although there was no obvious difference in the newly formed bone around implants among the three groups (Figure 6C), the percentage of BIC with the Lyo-Tre group (48.56%±5.52%) and Lyo-Tre-Lenti-EGFP group (47.12%±5.44%) was significantly higher than in the TiO_2 group ($P<0.01$; Figure 6D). By comparison, there was no statistical difference in the percentage of BIC between the Lyo-Tre and Lyo-Tre-Lenti-EGFP groups. Moreover, the Lyo-Tre-Lenti-BMP-2-EGFP group had the highest new bone area (0.21±0.02 mm^2) and BIC (65.32%±6.44%), which were both significantly higher than those values in the other three groups.

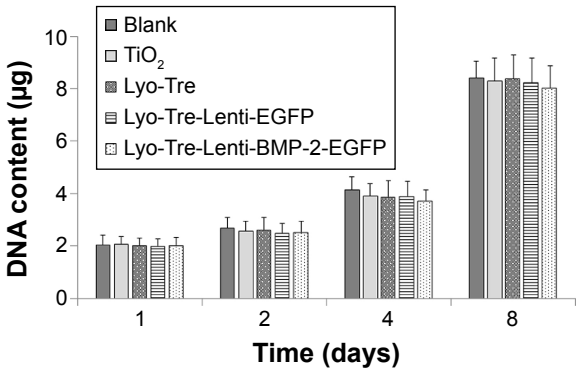

Figure 4 Effects of different nanotube formulations on BMSC proliferation.
Note: A DNA-based cell proliferation assay was used to analyze BMSCs cocultured with different nanotube types for 1, 2, 4, and 8 days.
Abbreviations: BMSC, bone marrow stromal cell; BMP, bone morphogenic protein.

Biomechanical testing

The results of the push-out test (expressed as the maximal push-out force) are shown in Figure 7, and a similar trend as the one seen in the BIC index result was observed among the groups. The Lyo-Tre-Lenti-BMP-2-EGFP group showed the highest failure load (110.33±12.61 N), while the TiO_2 group showed the lowest (48.91±5.13 N). In addition, the failure load values of the Lyo-Tre group (63.26±7.99 N) and Lyo-Tre-Lenti-EGFP group (61.95±7.18 N) were both higher than the TiO_2 group but less than that of the Lyo-Tre-Lenti-BMP-2-EGFP group. Furthermore, no statistical differences of the failure load values were observed between the two groups.

Discussion

Ti and its alloys have been widely studied in bone tissue engineering as substrates for cell attachment, differentiation, and ultimately osteogenesis because of their numerous advantages.[1] Previous results have shown that moderate TiO_2 nanotube layers on the Ti surface can enhance preosteoblast adhesion and differentiation.[5] As indicated in Figure 1, compared with the relatively smooth surface of pure Ti, TiO_2 nanotube layers were observable on the anodized Ti surface, suggestive of greater surface area and enhanced hydrophilicity. This would indicate an increased capacity for adsorbing biomolecules and cells to the surface, which could potentially prolong the time nanotubes are biologically active.[33] Meanwhile, when Lenti-BMP-2 was lyophilized onto TiO_2 nanotubes with addition of trehalose, an amorphous glassy matrix was visible on the surface of the anodized nanotube layers, and a decrease in uniformity and crystallinity was observed. Therefore, the nanometer surface roughness was also decreased. As previously described, compared with anatase-phase nanotube layers, amorphous nanotube layers with a tube diameter of >50 nm may partially impair mesenchymal stem cell growth at the initial stage.[34,35]

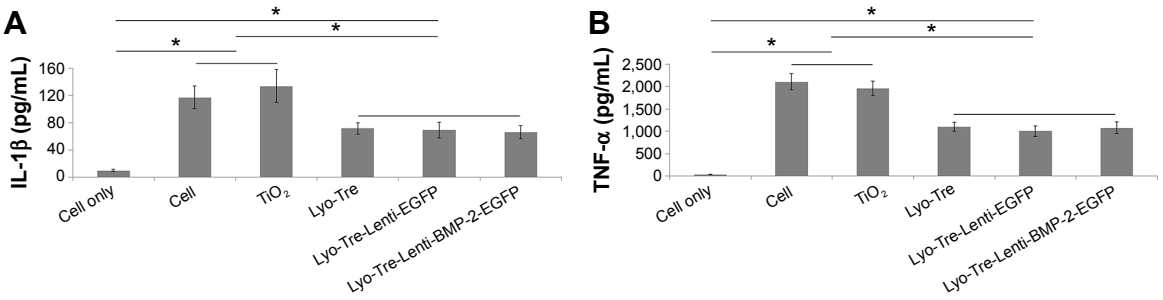

Figure 5 IL-1β (**A**) and TNF-α (**B**) production by RAW 264.7 cells incubated with different nanotube formulations.
Notes: Cell-free supernatants were collected at 12 hours, and IL-1β and TNF-α production was measured in ELISAs. The data are shown as mean ± SD. *$P<0.05$.
Abbreviations: BMP, bone morphogenic protein; IL-1β, interleukin-1β; TNF-α, tumor necrosis factor-α; ELISAs, enzyme-linked immunosorbent assays; SD, standard deviation.

However, after culture of 96 hours or more, cell proliferation rate was statistically similar for both amorphous and anatase nanotube layers, which is normally associated with cell proliferation period.[5]

In this work, we chose to use a lentiviral vector system for *BMP-2* gene transfer due to its numerous advantages.[20–22] However, lentiviral particles encoding BMP-2 tend to be easily inactivated by heat, extreme pH, or the presence of proteases, resulting in unstable activity during the desired therapeutic period.[20,21] Therefore, lyophilization was used in this study, which is an efficient approach widely used to improve the stability of various biomolecules,

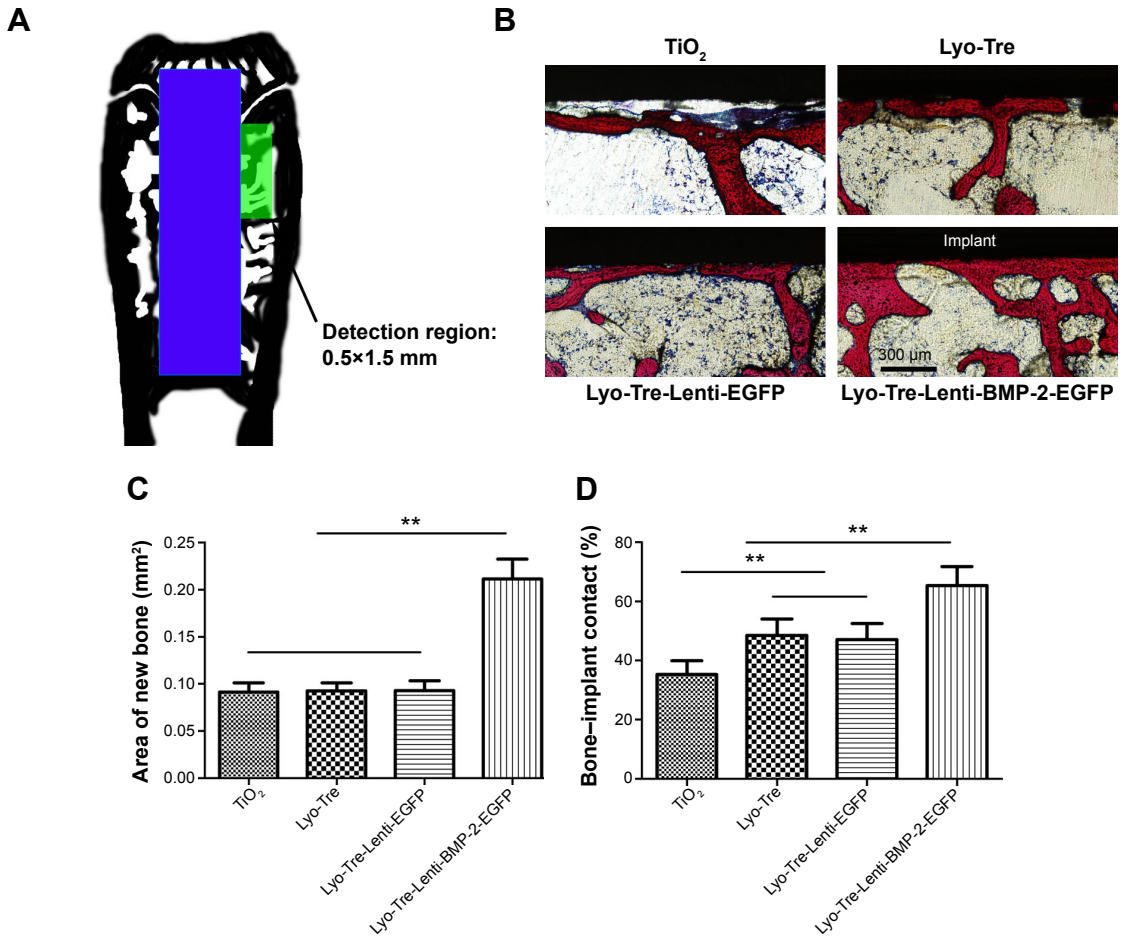

Figure 6 Histomorphometric observations of samples collected at week 8 after surgery.
Notes: (**A**) The image shows the green rectangle region that was selected to evaluate the new bone formation. The blue rectangle section is the implant inserted into the rat femur. (**B**) Histological observations of undecalcified sections stained with Van Gieson's picro fuchsin. (**C**) Results of newly formed bone area in the same region used for histological observations. (**D**) BIC results from the histomorphometric measurements. **$P<0.01$.
Abbreviations: BIC, bone–implant contact; BMP, bone morphogenic protein.

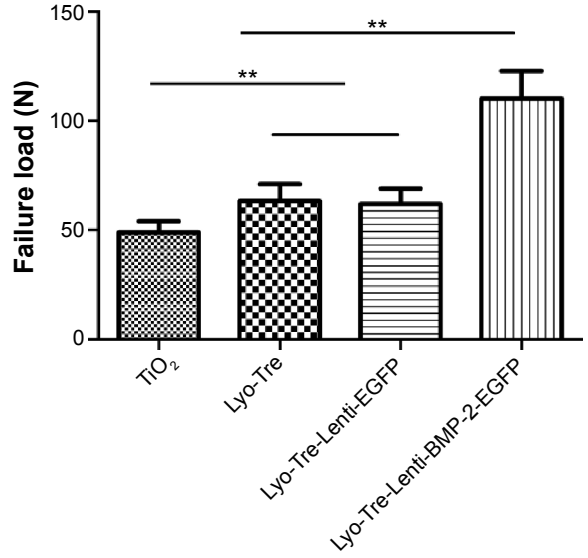

Figure 7 Biomechanical test results.
Note: $^{**}P<0.01$.
Abbreviation: BMP, bone morphogenic protein.

including viruses, proteins, peptides, and vaccines. Furthermore, lyophilization is an industrial process that removes water from a frozen sample by sublimation and desorption under vacuum, which enhances the immobilization of biomolecules on nanotubes.[36] This occurs as vacuum removes all traces of the solvent at a faster rate and loading occurs through a faster rate of biomolecule aggregation, with higher levels of physical adsorption. We found that when Lenti-BMP-2 was loaded onto TiO_2 nanotube layers by lyophilization with trehalose, the composite showed a slow release pattern (Figure 2A). This sustained release may be helpful for maintaining a high-localized growth factor concentration during the therapeutic period and for prolonging biological responses. To avoid the inactivation of biomolecules, we employed trehalose, which has been used to protect biostructures from damage due to dehydration, freezing, or heat exposure.[26,37] Trehalose was also released from the Lyo-Tre-Lenti-BMP-2-EGFP nanotubes (Figure 2B) gradually. This sustained release may induce a gentle decrease of trehalose and promote prolonged anti-inflammatory effects. With the Lyo-Tre-Lenti-EGFP and Lyo-Tre nanotubes, the trehalose-release profiles were similar to that observed with the Lyo-Tre-Lenti-BMP-2-EGFP nanotubes (data not shown).

Successful implants should not only support the attachment of cells to their surfaces but also promote osteogenic differentiation. Our results demonstrated that Lyo-Tre-Lenti-BMP-2-EGFP-modified anodic TiO_2 nanotube layers promoted the osteogenic differentiation of rat BMSCs (Figure 3). This observation may be explained by the sustained release of Lenti-BMP-2 into the microenvironment, which could infect neighboring BMSCs continuously, leading to stable BMP-2 production during the observation period. Furthermore, anodized TiO_2 nanotube layers have unique nanoscale structures; therefore, it is possible that the secreted BMP-2 peptide forms a unique structure on the nanotubes, thereby influencing the osteogenic differentiation of BMSCs.[38] We also found that the addition of trehalose to TiO_2 during lyophilization barely changed the osteogenic differentiation of BMSCs, suggesting that trehalose does not accelerate BMSCs osteogenesis.

Lyo-Tre-Lenti-BMP-2-EGFP-modified anodic TiO_2 nanotube layers did not promote BMSCs proliferation (Figure 4). It has been demonstrated that BMP-2 acts as a homing molecule to stimulate BMSCs homing,[39,40] and BMSCs from the bone marrow and other parts of the body can be triggered by implantation-related defect sites to enter the circulation.[41] Thus, we hypothesized that our delivery system may increase local cell accumulation by recruiting circulating BMSCs to implants, which in turn can induce their differentiation into osteoblasts.

Host-inflammatory responses to pathogens can lead to the destruction of implant-supporting tissues and cause implantation failures. More specifically, LPS produced by Gram-negative bacteria is a potent inducer of pro-inflammatory cytokines, such as IL-1β and TNF-α, which are critical mediators of pathogenesis. We found that IL-1β and TNF-α production was decreased in the presence of trehalose, compared with a positive control. These results indicated that trehalose can potentially block inflammatory responses[42] following implantation. Furthermore, a previous study also reported that trehalose suppresses osteoclast formation, which may be explained by the suppressive effects of trehalose on LPS-induced inflammatory cytokine production.[29] Although some researchers have studied their functional relationships,[28] the exact mechanism whereby trehalose suppresses inflammatory cytokine production remains unclear, and further studies on this subject are necessary. In comparison with the most common approaches for suppressing bacterial infections of implants using inorganic agents such as Cu, Zn, and Ag,[43] trehalose is a naturally occurring, nontoxic disaccharide that can preserve the activity of biomolecules and promote their sustained release from TiO_2 nanotubes. However, trehalose cannot inhibit the adhesion of bacteria, so finding a new substance having the advantages of both trehalose and inorganic chemical compositions will be an important area of future research.

For the evaluation of in vivo osseointegration, we employed Fisher 344 rats, which are commonly used for animal studies.

In our present study, at 8 weeks post-implantation, the obvious interspace between the newly formed bone and the implant surface was filled with fibrous tissue in the TiO_2 group, which could be partially attributed to inflammatory responses induced by the nanotube surface. This phenomenon was inconsistent with previous findings where, although TiO_2 nanotube layers improved bone formation and enhanced strongly adherent bone growth in vivo, nanotube surfaces caused inflammation.[9,44] On the other hand, TiO_2 nanotube layers did not inhibit cells proliferation (Figure 4), as previously described.[5,36] However, nano-debris could be generated at the bone–biomaterial interface when the TiO_2 nanotube implants were inserted into osseous tissue due to the mechanical damage, which could induce cytotoxicity.[45] This would be another reason. Compared with the other three groups (TiO_2, Lyo-Tre, and Lyo-Tre-Lenti-EGFP), the new bone area and BIC of the Lyo-Tre-Lenti-BMP-2-EGFP group were both significantly higher, in agreement with the push-out test results. We conclude that Lyo-Tre-Lenti-BMP-2-EGFP-modified anodic TiO_2 nanotube layers further promoted new bone formation surrounding the Ti implant and enhanced the osseointegration between the new bone and the implant surface by virtue of their enhanced osteogenic potential and anti-inflammatory properties.

Conclusion

In summary, improving the success rates of implant surgery remains a big challenge in various fields of medicine. Developing bioactive multifunctional coatings for implant surfaces appears to be a promising strategy for overcoming the limitations of current procedures. To the best of our knowledge, this work represents the first application of a combination of trehalose and lyophilization treatment to modify Ti-based implant surfaces with lentiviral particles encoding BMP-2, which can potentially promote enhanced osteogenesis and reduced inflammatory responses, simultaneously, to improve implant osseointegration. However, further long-term in vivo investigations are needed before their use in clinical applications can be realized.

Acknowledgment

This work was supported by the National Natural Science Foundation of China (grant numbers 81200815, 81000420, and 81271182).

Disclosure

None of the authors have conflicts of interest to declare.

References

1. Albrektsson T, Brånemark P-I, Hansson H-A, Lindström J. Osseointegrated titanium implants: requirements for ensuring a long-lasting, direct bone-to-implant anchorage in man. *Acta Orthop*. 1981;52(2):155–170.
2. Zhang W, Wang G, Liu Y, et al. The synergistic effect of hierarchical micro/nano-topography and bioactive ions for enhanced osseointegration. *Biomaterials*. 2013;34(13):3184–3195.
3. Le Guéhennec L, Soueidan A, Layrolle P, Amouriq Y. Surface treatments of titanium dental implants for rapid osseointegration. *Dent Mater*. 2007;23(7):844–854.
4. Buser D, Broggini N, Wieland M, et al. Enhanced bone apposition to a chemically modified SLA titanium surface. *J Dent Res*. 2004;83(7):529–533.
5. Yu Wq, Jiang Xq, Zhang Fq, Xu L. The effect of anatase TiO_2 nanotube layers on MC3T3-E1 preosteoblast adhesion, proliferation, and differentiation. *J Biomed Mater Res A*. 2010;94(4):1012–1022.
6. Kalbacova M, Rezek B, Baresova V, Wolf-Brandstetter C, Kromka A. Nanoscale topography of nanocrystalline diamonds promotes differentiation of osteoblasts. *Acta Biomater*. 2009;5(8):3076–3085.
7. Lamers E, Frank Walboomers X, Domanski M, et al. The influence of nanoscale grooved substrates on osteoblast behavior and extracellular matrix deposition. *Biomaterials*. 2010;31(12):3307–3316.
8. Oh S, Daraio C, Chen LH, Pisanic TR, Finones RR, Jin S. Significantly accelerated osteoblast cell growth on aligned TiO_2 nanotubes. *J Biomed Mater Res A*. 2006;78(1):97–103.
9. Bjursten LM, Rasmusson L, Oh S, Smith GC, Brammer KS, Jin S. Titanium dioxide nanotubes enhance bone bonding in vivo. *J Biomed Mater Res A*. 2010;92(3):1218–1224.
10. Le Nihouannen D, Komarova SV, Gbureck U, Barralet JE. Bioactivity of bone resorptive factor loaded on osteoconductive matrices: stability post-dehydration. *Eur J Pharm Biopharm*. 2008;70(3):813–818.
11. Wozney JM, Rosen V. Bone morphogenetic protein and bone morphogenetic protein gene family in bone formation and repair. *Clin Orthop Relat Res*. 1998;346:26–37.
12. Chen D, Zhao M, Mundy GR. Bone morphogenetic proteins. *Growth Factors*. 2004;22(4):233–241.
13. Yoon BS, Lyons KM. Multiple functions of BMPs in chondrogenesis. *J Cell Biochem*. 2004;93(1):93–103.
14. Baltzer A, Lieberman J. Regional gene therapy to enhance bone repair. *Gene Ther*. 2004;11(4):344–350.
15. Hsu W, Sugiyama O, Park S, et al. Lentiviral-mediated BMP-2 gene transfer enhances healing of segmental femoral defects in rats. *Bone*. 2007;40(4):931–938.
16. Jiang X, Zhao J, Wang S, et al. Mandibular repair in rats with premineralized silk scaffolds and BMP-2-modified bMSCs. *Biomaterials*. 2009;30(27):4522–4532.
17. Sugiyama O, An DS, Kung SP, et al. Lentivirus-mediated gene transfer induces long-term transgene expression of BMP-2 in vitro and new bone formation in vivo. *Mol Ther*. 2005;11(3):390–398.
18. Naldini L, Blömer U, Gallay P, et al. In vivo gene delivery and stable transduction of nondividing cells by a lentiviral vector. *Science*. 1996;272(5259):263–267.
19. Zufferey R, Dull T, Mandel RJ, et al. Self-inactivating lentivirus vector for safe and efficient in vivo gene delivery. *J Virol*. 1998;72(12):9873–9880.
20. Mozhaev VV. Mechanism-based strategies for protein thermostabilization. *Trends Biotechnol*. 1993;11(3):88–95.
21. Arakawa T, Prestrelski SJ, Kenney WC, Carpenter JF. Factors affecting short-term and long-term stabilities of proteins. *Adv Drug Deliv Rev*. 2001;46(1):307–326.
22. Wang W. Lyophilization and development of solid protein pharmaceuticals. *Int J Pharm*. 2000;203(1):1–60.
23. Abdelwahed W, Degobert G, Stainmesse S, Fessi H. Freeze-drying of nanoparticles: formulation, process and storage considerations. *Adv Drug Deliv Rev*. 2006;58(15):1688–1713.

24. Griebenow K, Klibanov AM. Lyophilization-induced reversible changes in the secondary structure of proteins. *Proc Natl Acad Sci U S A*. 1995;92(24):10969–10976.
25. Kasper JC, Schaffert D, Ogris M, Wagner E, Friess W. Development of a lyophilized plasmid/LPEI polyplex formulation with long-term stability – a step closer from promising technology to application. *J Control Release*. 2011;151(3):246–255.
26. Lins RD, Pereira CS, Hünenberger PH. Trehalose–protein interaction in aqueous solution. *Proteins*. 2004;55(1):177–186.
27. Neta T, Takada K, Hirasawa M. Low-cariogenicity of trehalose as a substrate. *J Dent*. 2000;28(8):571–576.
28. Taya K, Hirose K, Hamada S. Trehalose inhibits inflammatory cytokine production by protecting IκB-α reduction in mouse peritoneal macrophages. *Arch Oral Biol*. 2009;54(8):749–756.
29. Arai C, Kohguchi M, Akamatsu S, et al. Trehalose suppresses lipopolysaccharide-induced osteoclastogenesis bone marrow in mice. *Nutr Res*. 2001;21(7):993–999.
30. Lois C, Hong EJ, Pease S, Brown EJ, Baltimore D. Germline transmission and tissue-specific expression of transgenes delivered by lentiviral vectors. *Science*. 2002;295(5556):868–872.
31. Zhao J, Hu J, Wang S, et al. Combination of β-TCP and BMP-2 gene-modified bMSCs to heal critical size mandibular defects in rats. *Oral Dis*. 2010;16(1):46–54.
32. Rage R, Mitchen J, Wilding G. DNA fluorometric assay in 96-well tissue culture plates using Hoechst 33258 after cell lysis by freezing in distilled water. *Anal Biochem*. 1990;191(1):31–34.
33. Webster TJ, Siegel RW, Bizios R. Osteoblast adhesion on nanophase ceramics. *Biomaterials*. 1999;20(13):1221–1227.
34. Park J, Bauer S, von der Mark K, Schmuki P. Nanosize and vitality: TiO_2 nanotube diameter directs cell fate. *Nano Lett*. 2007;7(6):1686–1691.
35. Bauer S, Park J, von der Mark K, Schmuki P. Improved attachment of mesenchymal stem cells on super-hydrophobic TiO_2 nanotubes. *Acta Biomater*. 2008;4(5):1576–1582.
36. Zhang W, Jin Y, Qian S, et al. Vacuum extraction enhances rhPDGF-BB immobilization on nanotubes to improve implant osseointegration in ovariectomized rats. *Nanomedicine*. 2014;10(8):1809–1818.
37. Crowe JH, Carpenter JF, Crowe LM. The role of vitrification in anhydrobiosis. *Annu Rev Physiol*. 1998;60(1):73–103.
38. Sun S, Yu W, Zhang Y, Zhang F. Increased preosteoblast adhesion and osteogenic gene expression on TiO_2 nanotubes modified with KRSR. *J Mater Sci Mater Med*. 2013;24(4):1079–1091.
39. Fiedler J, Röderer G, Günther KP, Brenner RE. BMP-2, BMP-4, and PDGF-bb stimulate chemotactic migration of primary human mesenchymal progenitor cells. *J Cell Biochem*. 2002;87(3):305–312.
40. Zhang W, Zhu C, Wu Y, et al. VEGF and BMP-2 promote bone regeneration by facilitating bone marrow stem cell homing and differentiation. *Eur Cell Mater*. 2014;27(1):1–11.
41. Chen F-M, Wu L-A, Zhang M, Zhang R, Sun H-H. Homing of endogenous stem/progenitor cells for in situ tissue regeneration: promises, strategies, and translational perspectives. *Biomaterials*. 2011;32(12):3189–3209.
42. Yoshizane C, Arai N, Arai C, et al. Trehalose suppresses osteoclast differentiation in ovariectomized mice: correlation with decreased in vitro interleukin-6 production by bone marrow cells. *Nutr Res*. 2000;20(10):1485–1491.
43. Qian S, Qiao Y, Liu X. Selective biofunctional modification of titanium implants for osteogenic and antibacterial applications. *J Mater Chem B*. 2014;2(43):7475–7487.
44. Chamberlain L, Brammer K, Johnston G, Chien S, Jin S. Macrophage inflammatory response to TiO_2 nanotube surfaces. *J Biomater Nanobiotechnol*. 2011;2(3):293–300.
45. Zhang Y, Yu W, Jiang X, Lv K, Sun S, Zhang F. Analysis of the cytotoxicity of differentially sized titanium dioxide nanoparticles in murine MC3T3-E1 preosteoblasts. *J Mater Sci Mater Med*. 2011;22:1933–1945.